First-order visual interneurons distribute distinct contrast and luminance information across ON and OFF pathways to achieve stable behavior

Madhura Ketkar*[1,2], Burak Gür*[1,2], Sebastian Molina-Obando*[1,2], Maria Ioannidou[1,3], Carlotta Martelli[1] and Marion Silies[1]

[1] Institute of Developmental Biology and Neurobiology, Johannes-Gutenberg University Mainz, 55128 Mainz, Germany.

[2] Göttingen Graduate School for Neurosciences, Biophysics, and Molecular Biosciences (GGNB) and International Max Planck Research School (IMPRS) for Neurosciences at the University of Göttingen, 37077 Göttingen, Germany

[1,3] Present address: School of Physics, Faculty of Sciences, Aristotle University of Thessaloniki, 54124, Greece

* these authors contributed equally to this work

Corresponding author: msilies@uni-mainz.de

Abstract

The accurate processing of contrast is the basis for all visually guided behaviors. Visual scenes with rapidly changing illumination challenge contrast computation, because adaptation is not fast enough to compensate for such changes. Yet, human perception of contrast is stable even when the visual environment is quickly changing. The fruit fly Drosophila also shows nearly luminance invariant behavior for both ON and OFF stimuli. To achieve this, first-order interneurons L1, L2 and L3 all encode contrast and luminance differently, and distribute information across both ON and OFF contrast-selective pathways. Behavioral responses to both ON and OFF stimuli rely on a luminance-based correction provided by L1 and L3, wherein L1 supports contrast computation linearly, and L3 non-linearly amplifies dim stimuli. Therefore, L1, L2 and L3 are not distinct inputs to ON and OFF pathways but the lamina serves as a separate processing layer that distributes distinct luminance and contrast information across ON and OFF pathways to support behavioral performance in varying conditions.

Introduction

Across species, contrast information forms the basis of visual computations. For our perception to be stable, our eyes must compute contrast relative to the mean illumination of a scene. In natural environments, illumination changes by several orders of magnitude not only from dawn to dusk, but also at much faster timescales as our eyes saccade across a scene or we quickly move from sun to shade (Frazor and Geisler, 2006; Mante et al., 2005; Rieke and Rudd, 2009).Thus, the computation of contrast needs to be invariant to rapid changes in luminance, such that visual perception of a given contrast remains constant. This is accomplished by human perception, and neuronal responses in the cat lateral geniculate nucleus (LGN) display contrast constancy at rapid time scales (Burkhardt et al., 1984; Mante et al., 2005). However, contrast encoding in photoreceptors is not luminance invariant when the stimulus changes more rapidly than photoreceptor adaptation (Laughlin and Hardie, 1978; Normann and Werblin, 1974).

The visual OFF pathway in fruit flies, sensitive to contrast decrements, also displays contrast-constant behavior (Ketkar et al., 2020) , allowing to investigate the underlying mechanisms. In the OFF pathway, luminance information itself is maintained postsynaptic to photoreceptors, and is crucial for the accurate estimation of contrast, resulting in contrast-constant behavior. Luminance serves as a corrective signal that scales contrast computation when background luminance quickly changes (Ketkar et al., 2020). The requirement of such a corrective signal can be theoretically expected regardless of ON and OFF contrast polarities, since the adaptational constraints in dynamic environments challenge both contrast polarities. However, the ON and OFF pathways are not mere sign-inverted versions of each other since they face different environmental challenges (Clark et al., 2014; Ruderman, 1994) and have evolved several structural and physiological asymmetries (Chichilnisky and Kalmar, 2002; Jin et al., 2011; Leonhardt et al., 2016; Ratliff et al., 2010). It is thus not clear if this luminance invariance is a general feature of all visual pathways, and how luminance and contrast information are distributed across visual pathways to establish contrast constancy is not known.

Drosophila melanogaster offers a promising model system to study the pathway-specific function of luminance since the ON and OFF motion pathways have been well characterized on the cellular, circuit and behavioral levels (Behnia et al., 2014; Yang and Clandinin, 2018). In the fly visual system, neurons were assigned to distinct ON or OFF pathways based on physiological properties (Molina-Obando et al., 2019; Serbe et al., 2016; Shinomiya et al., 2019; Silies et al., 2013; Strother et al., 2017), anatomical connectivity (Shinomiya et al., 2014; Takemura et al., 2015, 2013, 2017), and behavioral function (Clark et al., 2011; Silies et al., 2013). ON and OFF contrast selectivity first arises two synapses downstream of photoreceptors, in medulla neurons (Fischbach and Dittrich, 1989; Serbe et al., 2016; Silies et al., 2013; Strother et al., 2017; Yang et al., 2016). They receive photoreceptor information through the lamina neurons L1-L3, which project to specific medulla layers (Meinertzhagen and O'Neil, 1991; Strother et al., 2014). Although L1-L3 all show the same response polarity, and hyperpolarize to light onset and depolarize to light offset, L1 projects to layers where it mostly connects to ON-selective medulla neurons. Similarly, L2 and L3 project to layers where OFF-selective medulla neurons get most of their inputs (Shinomiya et al., 2014; Takemura et al., 2015, 2013). L1 is thus thought to be the

sole major input of the ON pathway, whereas L2 and L3 are considered the two major inputs of the OFF pathway (Figure 1A) (Clark et al., 2011; Joesch et al., 2008; Shinomiya et al., 2019). Among these, L2 is contrast-sensitive, but cannot support contrast constancy alone if photoreceptor adaptation is insufficient. Instead, contrast constancy in OFF-motion guided behavior is ensured by a corrective signal from luminance-sensitive L3 neurons (Ketkar et al., 2020). It is not known whether ON-motion driven behavior also requires luminance information and whether L1 can provide it along with its contrast signal (Figure 1B).

Contrast and luminance are both encoded by the transient and sustained response components in both vertebrates and invertebrate photoreceptors (Laughlin and Hardie, 1978; Normann and Perlman, 1979; Normann and Werblin, 1974; Shapley and Enroth-Cugell, 1984), which are captured differentially by their downstream neurons. In the vertebrate retina, many different types of first order interneurons, bipolar cells, exist. Although they are generally thought to capture the contrast component of the photoreceptors response, luminance information has been shown be preserved in post-photoreceptor visual circuitry post of the retina (Awatramani and Slaughter, 2000; Ichinose and Hellmer, 2016; Ichinose and Lukasiewicz, 2007; Odermatt et al., 2012; Oesch and Diamond, 2011). As suggested by their sustained response component, different degrees of luminance-sensitivity exists across bipolar cell types (Baden et al., 2016; Euler et al., 2014). Furthermore, ON and OFF contrast selectivity emerges at the bipolar cell layer, where ON selectivity emerges through glutamatergic inhibition (Masu et al., 1995). These ON and OFF bipolar cells also split anatomically, as they innervate different layers (Euler et al., 2014).
Together, many parallels exist between the Drosophila visual system and the vertebrate retina, including the response properties of photoreceptors, the layered organization and the existence of ON and OFF pathways (Clark and Demb, 2016; Mauss et al., 2017). However, in contrast to the vertebrate retina, fewer first order interneuron types distribute contrast and luminance information, and contrast selectivity itself clearly only occurs one synapse further downstream, where neurons postsynaptic to lamina neurons are either ON or OFF selective. Comparing the vertebrate retina with the insect visual system, it is unclear how just three first order interneurons distribute their different physiological properties across visual pathways.

Here, we show that luminance and contrast information is distributed to, and is of behavioral relevance for both ON and OFF pathways. In vivo calcium imaging experiments reveal that each first order interneuron is unique in its contrast and luminance encoding properties. Whereas L2 is purely contrast sensitive, L1 encodes both contrast and luminance in distinct response components. L1 linearly scales with luminance, whereas the luminance-sensitive L3 non-linearly amplifies dim light. Behavioral experiments further show that these differential luminance- and contrast- encoding properties translate into distinct behavioral roles. In the ON pathway, L1 and L3 both provide luminance information for higher luminance invariance than possible by the contrast input alone. Furthermore, L2, known as the OFF-pathway contrast input, provides contrast information to the ON-pathway, in addition to L1. Surprisingly, both L1 and L3 neurons are necessary and sufficient for OFF behavior. These findings indicate that L1 L2, and L3 do not constitute ON- or OFF-specific inputs. Instead, the three first-order interneurons encode luminance and contrast differentially and contribute to computations in both ON and OFF pathways. Together, our data reveal how luminance and contrast information are distributed to

both ON and OFF pathways to approach luminance invariance, a core computation of visual systems.

Results

L1 responses to contrast do not explain ON behavior

Luminance-invariant behavioral responses have been observed in multiple species (Burkhardt et al., 1984; Silies et al., 2014), highlighting their ethological relevance. In *Drosophila*, luminance-invariant behavior has been shown in response to OFF stimuli, where a dedicated luminance-sensitive pathway scales contrast-sensitive inputs to achieve luminance invariance in behavior (Ketkar et al., 2020). The ON pathway is thought to have just one prominent input, L1. We thus asked if luminance invariance is achieved in the ON pathway and if the contrast-sensitive input L1 can explain such invariance. For this purpose, we compared turning behavior of walking flies with the responses of L1. Behavioral responses were measured in a fly-on-a-ball assay. Flies were shown moving ON edges of different luminance but the same 100% Michelson contrast. Fly turning responses were highly similar across luminances, with low-luminance edges eliciting slightly larger turning responses than brighter edges (Figure 1C).

We wondered if the sole ON pathway input L1 can directly drive this behavior. To test this, we examined the contrast responses of L1 to moving ON edges with comparable parameters and overlapping luminance values as those used in the behavioral assay (Figure 1D). We recorded L1 *in vivo* calcium responses to visual stimuli from its axon terminals expressing GCaMP6f using two-photon microscopy. As described previously, L1 responded negatively to contrast increments, in line with the inverted response polarity of lamina neurons (Figure 1D) (Clark et al., 2011; Laughlin and Hardie, 1978; Yang et al., 2016). The absolute response amplitude of the L1 calcium signals scaled with luminance and did not co-vary with the behavioral response (Figure 1E). We performed linear regression across calcium signals at different luminances and quantified the slope to extract the luminance dependency of the responses. L1 signals and behavioral responses had opposite luminance dependencies (Figure 1E). Thus, the observed behavior, approaching luminance invariance, cannot be explained solely by contrast inputs from L1, suggesting that the ON-pathway additionally gets luminance-sensitive input.

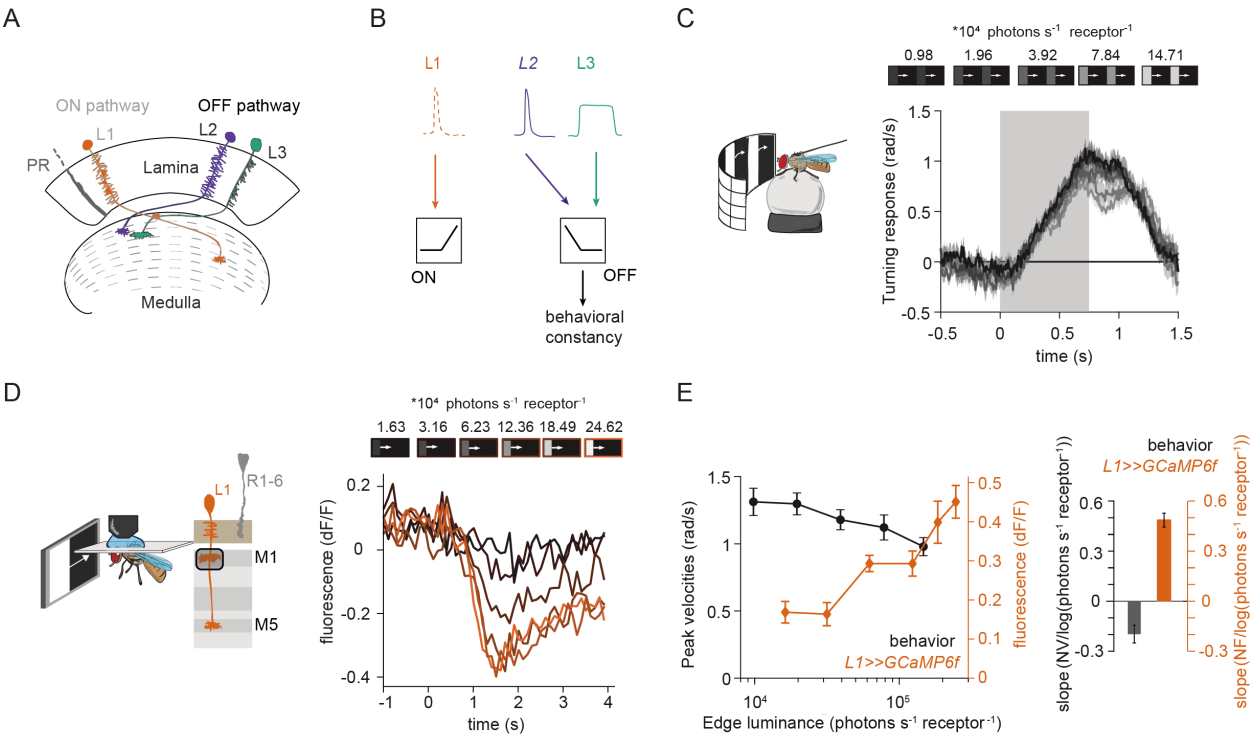

Figure 1: L1 responses to contrast do not explain ON behavior across luminance. (A) Schematic of lamina neurons projecting from the lamina to the medulla . L1 is considered the main input to the ON-pathway, whereas L2 and L3 are thought to provide input to the OFF pathway. **(B)** Transient L2 and sustained L3 neurons provide contrast and luminance information, respectively, to the OFF pathway to guide contrast-constant behavior (Ketkar et al., 2020). L1 is thought to have physiological properties very similar to L2 (Clark et al., 2011) and provides contrast information to the ON selective pathway. **(C)** Turning response to multiple moving ON edges, displayed on an LED arena that surrounds a fly walking on an air-cushioned ball. The edge luminance takes five different values, and the background is dark (~0 luminance), all resulting in 100% contrast. Turning responses are color-coded according to the edge luminance. The gray box indicates motion duration. n = 10 flies. **(D)** *In vivo* calcium signals of L1 axon terminal in medulla layer M1 in response to moving ON edges of six different luminances. Calcium responses of single L1 axon terminal are shown. **(E)** Left: Absolute step responses of L1 are plotted together with peak turning velocities calculated from (C). Behavioral and calcium traces are aligned by maximum response. Right, slope quantification of luminance dependency for normalized behavior and L1 fluorescence signals. NV = normalized peak velocity, NF = normalized fluorescent signal. Traces and plots in C and E show mean ± SEM.

L1 neuronal responses carry a luminance-sensitive component

To explore the sources of luminance information in first-order interneurons, we measured calcium signals in L1, L2 and L3. Flies were shown a staircase stimulus with luminance going sequentially up and down. L1 and L2 showed positive and negative transient responses when luminance stepped down and up, respectively (Figure 2A), consistent with their contrast sensitivity (Clark et al., 2011; Silies et al., 2013). L2 did not show any sustained component. L3 showed sustained responses to OFF steps and was non-linearly tuned to stimulus luminance, responding strongly to the darkest stimulus. Intriguingly, L1 showed a transient component followed by a sustained component, suggesting that it encodes luminance in addition to contrast (Figure 2A). The sustained components of L1 response were negatively correlated with luminance, such that the baseline calcium signal at each step sequentially increased with decreasing stimulus luminance.

Thus, in addition to L3, L1 also maintains luminance information postsynaptically to photoreceptors.

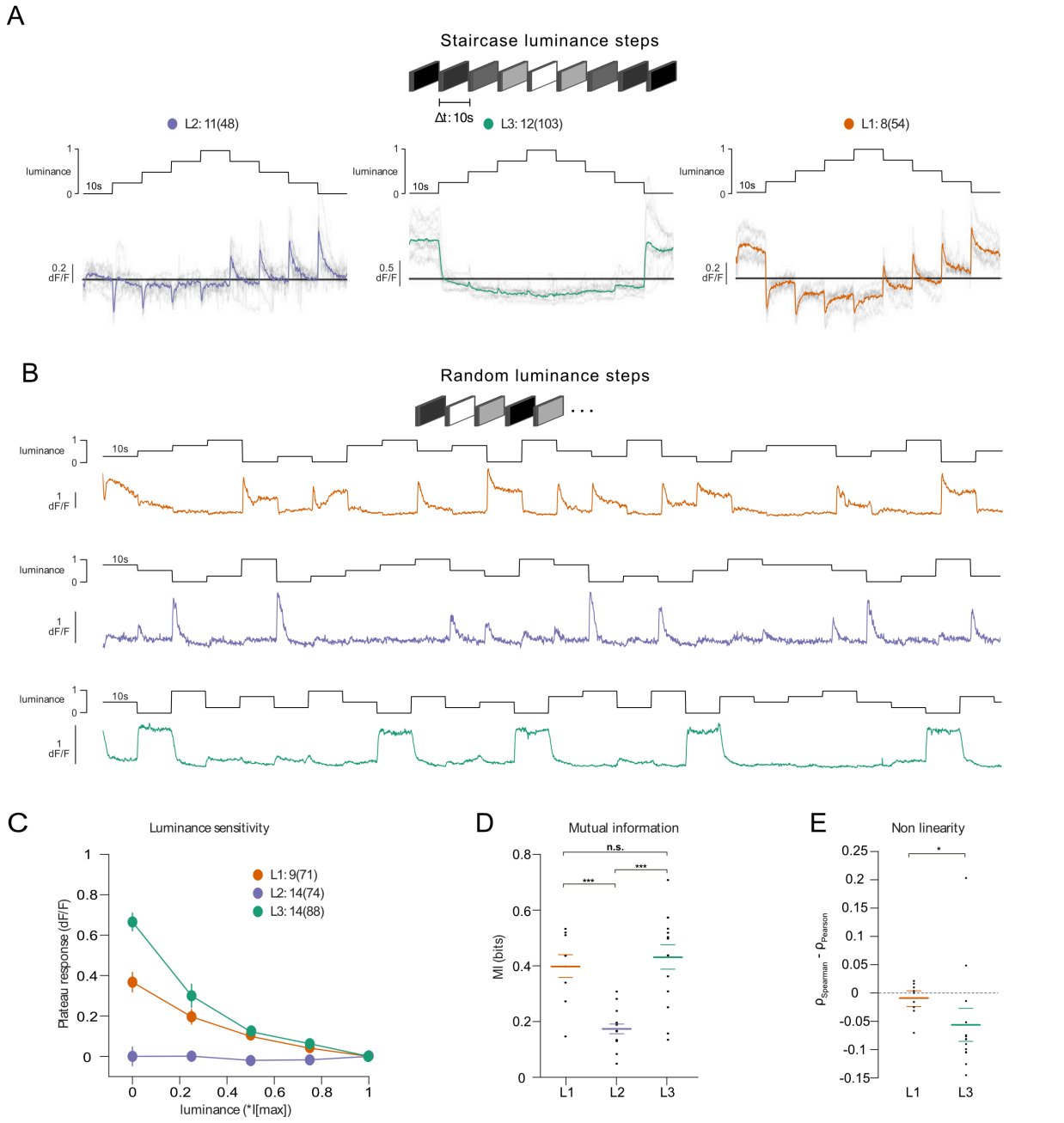

Figure 2: Lamina neuron types L1-L3 are differently sensitive to contrast and luminance. (A) Schematic of the 'staircase' stimulus. Luminance sequentially steps up through five values and then sequentially steps down. Shown below are the plateau calcium responses of L1 (orange), L2 (purple) and L3 (green) axon terminals, plotted against luminance. Colored traces shown the mean response, grey traces show individual fly means. (B) Example calcium traces of single L1, L2 and L3 axon terminals to a stimulus comprising 10 s full-field flashes varying randomly between five different luminances. (C) Plateau responses of the three neuron types, quantified from the responses to the stimulus in (B). (D) Mutual information between luminance and calcium signal, ***p < 0.001, one-way ANOVA followed by multiple comparison test corrected with Bonferroni. (E) Non-linearity quantification of luminance-dependent signals of L1 and L3 in (C), *p < 0.05, tested by a wilcoxon rank sum test.

To explicitly compare luminance information across the three input neurons, we measured responses to randomized luminance and calculated the mutual information between stimulus and the sustained response component (Figure 2B-D). As for the staircase stimulus, L2 transient responses returned to baseline within the 10s of the stimulus presentation, whereas both L1 and L3 displayed sustained components that varied with luminance (Figure 2B,C). Sustained response components in L1 and L3 carried similar mutual information with luminance, and both were higher than L2 (Figure 2D). Interestingly, the luminance-sensitive response components of L1 and L3 scaled differently with luminance. We quantified non-linearity using the difference of Pearson's linear and Spearman's correlation between response and luminance. This value will approach zero if the relationship is linear and increase or decrease if non-linear, depending on the sign of correlation between luminance and response. L1 responses were more linear with respect to luminance than L3 responses, which selectively amplified low luminance (Figure 2E). Thus, the two luminance-sensitive neurons carry different types of luminance information.

L1 is not required but sufficient for ON behavior across luminances

Since the canonical ON pathway input L1 is also found to carry luminance information, we hypothesized that it plays a role in mediating the observed behavior. To test this, we silenced L1 outputs while measuring ON behavior using Shibire^{ts} (Kitamoto, 2001). Silencing L1 severely reduced turning responses when different ON contrasts were interleaved, consistent with previous behavioral studies that identified L1 as the major input to the ON pathway (Clark et al., 2011; Silies et al., 2013) (Supp. Figure 1A-D). However, L1 silencing had little effect on responses to 100% contrast at varying luminance, suggesting the existence of other ON pathway inputs (Figure 3A,B). To explicitly test if and how L1 silencing changed the luminance dependence of behavioral responses, we quantified the slope of peak turning velocities across different background luminances (Figure 3C). The slopes were slightly negative for both the control and L1-silenced conditions, and did not differ significantly between conditions, suggesting another luminance input masking the L1 contribution. To test this possibility, we asked if L1 is sufficient for ON behavior in dynamically changing luminance conditions. We measured behavioral responses after functionally isolating L1 from other circuitry downstream of photoreceptors. To achieve this, we selectively rescued expression of the histamine-gated chloride channel Ort in *ort*-mutant flies, which otherwise lack communication between photoreceptors and their postsynaptic neurons. Behavioral responses of *ort* mutant control flies were absent, indicating that ON-motion behavior fully depends on Ort (Figure 3D). Heterozygous *ort* controls turned with the moving 100% contrast ON edges at all luminances (Figure 3E). Flies in which *ort* expression was rescued in L1 responded to ON motion at all luminances, and indistinguishable from controls (Figure 3F), showing that L1 can mediate normal turning behavior to ON edges at all luminances. This data confirms L1's general importance in the ON pathway and additionally highlights its behaviorally relevant role of its luminance-sensitive component.

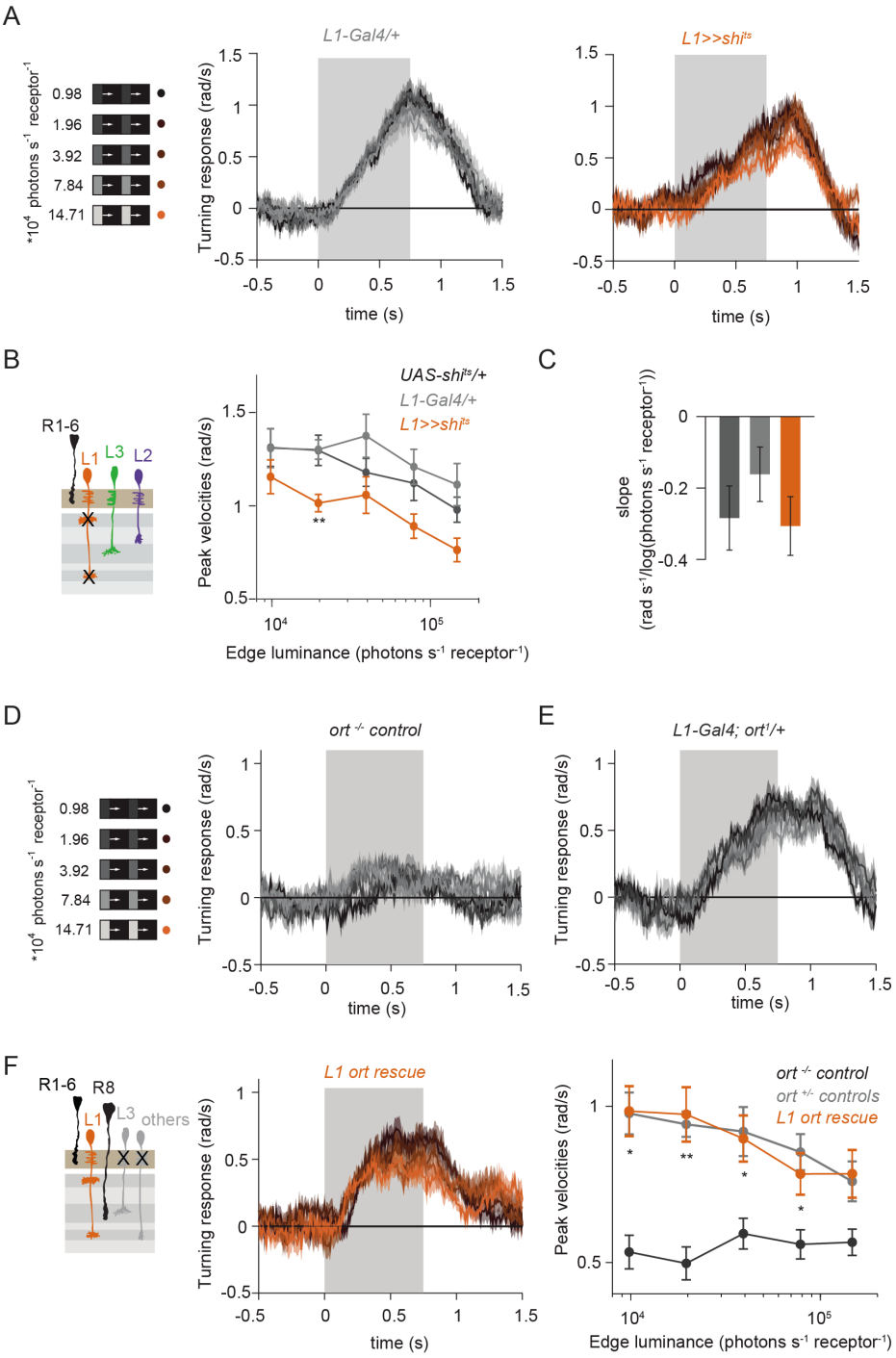

Figure 3: L1 is not required but sufficient for ON behavior across luminance. (A) Turning responses of L1-silenced flies (blue) and their specific Gal4 control (gray) to moving 100% contrast ON edges at five different luminances. (B) Peak velocities quantified for each of the five edges during the motion period, also including the control *UAS-shi^{ts}*/+, **p < 0.01, two-tailed Student's t tests against both controls. (C) Relationship of the peak velocities with luminance, quantified as slopes of the linear fits to the data in (B). Sample sizes are n = 10 flies for each genotype. (D-E) Schematic of the stimulus (same as in A) and turning responses of the *ort* null mutant (*ort$^{-/-}$* controls, D) and heterozygous *ort* controls (*ort$^{+/-}$*controls, E). (F) Schematic of the L1 ort rescue genotype and turning responses of L1 ort rescue flies (left). Peak turning velocities of L1 ort rescue flies and the respective controls (right); *p<0.05, **p < 0.01, two-tailed Student's t tests against both controls. The gray box region in (A,D,E,F) indicates motion duration. Traces and plots show mean ± SEM.

L1 and L3 together provide luminance signals required for ON behavior

Our data suggest the existence of a second luminance input to the ON-pathway. In the OFF pathway, the luminance-sensitive L3 neuron provides the necessary luminance-based correction to achieve contrast constancy (Ketkar et al., 2020). Connectomics data suggest that L3 could provide input to the ON pathway as well (Takemura et al., 2013). To test the hypothesis that L3 also provides a luminance signal to approach luminance-invariant ON responses, we measured behavioral responses to a set of 100% contrast ON edges at five different luminances while silencing L3 synaptic outputs (Figure 4A,B). Interestingly, unlike controls, L3-silenced flies responded stronger to all ON edges, revealing an unexplored, inhibitory role of L3. However, the responses of L3-silenced flies were still highly similar across luminances. This demonstrates that, like L1, L3 is not alone required for the near-invariant ON pathway behavior. Unlike controls, L3 silenced flies did not show a slight increase in turning amplitude at lower edge luminance, also reflected in the differences in their slopes (Figure 4C), suggesting that L3 inputs to the ON pathway also contribute to behavior in a luminance-dependent manner. To further explore this, we next asked if L3 is sufficient for ON behavior and functionally isolated L3 from other circuitry. L3 rescue flies turned to ON edges at all luminances tested (Figure 4D) and significantly rescued turning behavior at low luminances compared to *ort* mutant flies (Figure 4E), showing that L3 is sufficient for ON behavior at low luminances. This further reflects L3's nonlinear preference for dim light seen at the physiological level (Ketkar et al., 2020), (Figure 2C).

We found that L3 is a second luminance input to the ON-pathway that, together with L1, supports luminance-invariant responses in ON behavior. To test this, we silenced the outputs of both L1 and L3 simultaneously while measuring ON behavior across luminance. Flies still turned to the moving ON edges. However, turning responses of flies lacking both L1 and L3 functional outputs were no longer luminance invariant and turned less than controls in a luminance-dependent manner (Figure 4F,G). Intriguingly, behavioral responses now scaled positively with the edge luminance (Figure 4H), qualitatively recapitulating the LMC contrast-sensitive responses. Thus, L1 and L3 can together account for the luminance information available to the ON pathway. To analyze the extent of the individual contributions of L1 and L3, we compared L1 and L3 ort rescues by computing rescue efficiency, defined as the fraction of the difference between positive and negative control behaviors. Whereas L1 fully rescued turning behavior to ON edges at all luminances, L3 significantly rescued turning behavior selectively at low luminances (Figure 4I). Taken together, L1 and L3 both provide distinct types of luminance information to the ON pathway (Figure 4J). Because flies lacking both of these neurons still respond to ON contrast, our data suggest the existence of an unidentified contrast input.

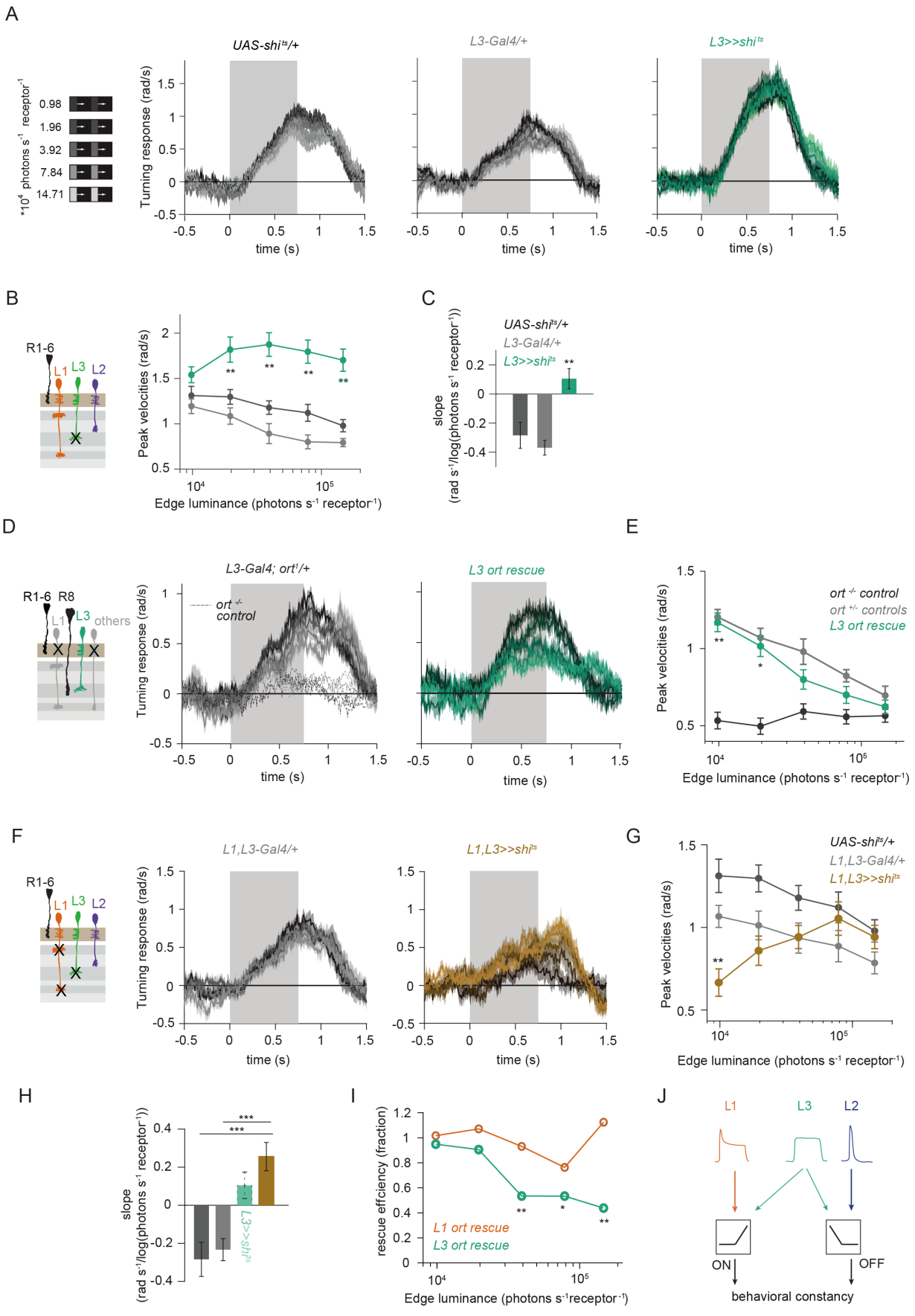

280

Figure 4: L1 and L3 together provide luminance signals required for ON behavior. (A) Turning velocities of the controls (gray) and L3-silenced flies (green) in response to five moving ON edges of 100% contrast . The gray box region indicates motion duration. (B) Peak turning velocities for five ON edges quantified during the motion period, **p < 0.01, two-tailed Student's t tests against both controls. (C) Relationship of the peak velocities with luminance, quantified as slopes of the linear fits to the data in (B). Fitting was done for individual flies. Sample sizes are n = 10 (*UAS-shi^{ts}/+,L3>>shi^{ts}*) and n = 8 (*L3^{0595}-Gal4/+*). (D) Schematic of the L3 *ort* rescue genotype and turning responses of the heterozygous control (gray) and rescue (green) flies. (E) Peak turning velocities, *p<0.05, **p < 0.01, two-tailed Student's t tests against both controls. (F) Turning responses of flies where L1 and L3 were silenced together (golden brown) and their specific Gal4 control (gray), color-coded according to ON edge luminance. The same five moving ON edges of 100% contrast as in Figure 2A were shown. Responses of the other control *UAS-shi^{ts}/+* to these stimuli have been included in Figure 1C. (G) Peak velocities quantified for each of the five edges during the motion period, also including the control *UAS-shi^{ts}/+*, **p < 0.01, two-tailed Student's t tests against both controls. (H) Relationship of the peak velocities with luminance, quantified as slopes of the linear fits to the data in (G). Slopes from the L3-silenced flies (green, dashed) responding to the same stimuli (Figure 3C) are included again for comparison. Fitting was done for individual flies. Sample sizes are n = 10 (*UAS-shi^{ts}/+*and *L1,L3>>shi^{ts}*) and n = 7 (*L1^{c2025}-Gal4/+;L3^{0595}-Gal4/+*). (I) Efficiency of the L1 and L3 behavioral rescue, calculated for each edge luminance as (*rescue - ort$^{-/-}$ control*) / (*ort$^{+/-}$ control - ort$^{-/-}$* control). *p<0.05, **p < 0.01, permutation test with 1000 permutations over the *L1 ort rescue* and *L3 ort rescue* flies. (J) Summary schematic. The ON pathway in addition to the OFF pathway receives a prominent input from L3. Like the OFF pathway, the ON pathway drives contrast constant behavior. Traces and plots show mean ± SEM.

The contrast-sensitive L2 provides input to the ON-pathway

Besides L1 and L3, the remaining input downstream of photoreceptors is the contrast-sensitive L2 neuron, which provides strong inputs to OFF-pathway neurons (Takemura et al., 2013). To explore the possibility of L2 also being an ON pathway input, we silenced L2 outputs either individually or together with L1. L2-silenced flies showed only slightly reduced turning to all ON edges as compared to controls (Figure 5A,B) similarly to silencing L1 alone (Figure 3A,B). However, when L1 and L2 were silenced together, fly turning responses were fully disrupted across conditions (Figure 5C,D). Moreover, these flies did not turn to other ON contrasts steps either (Supp. Figure 2). This shows that L2, together with L1, is required for ON behavioral responses across different contrasts and luminances. Altogether, L1, L2 and L3 are all ON-pathway inputs.

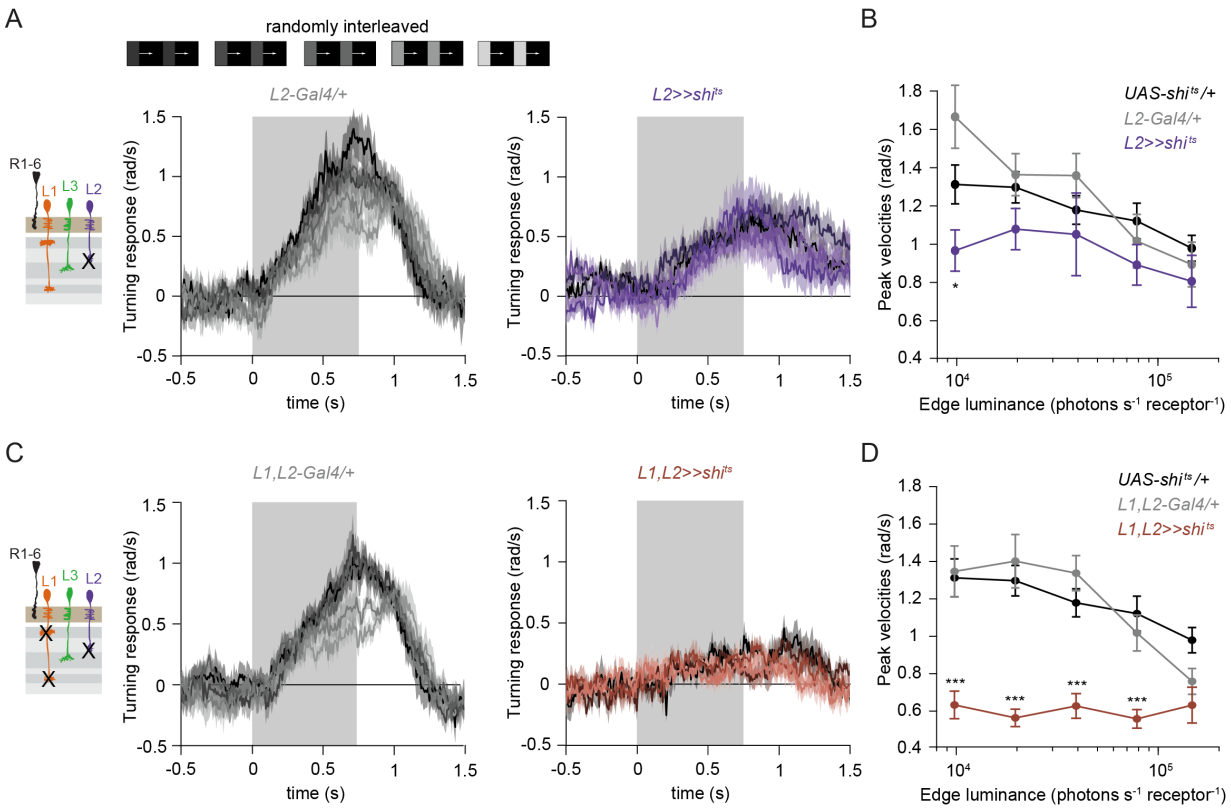

Figure 5: The contrast-sensitive L2 provides input to the ON-pathway. (A) Turning responses of flies where L2 was silenced (purple) and their specific Gal4 control (gray), color-coded according to 100% contrast ON edge at five different luminances. Sample sizes are n = 9 (*L2^{21Dhh}>>shi^{ts}*) and n = 6 (*L2^{21Dhh}-Gal4/+*). (B) Peak velocities quantified for each of the five edges during the motion period, *p < 0.05, two-tailed Student's t tests against both controls. (C) Turning responses of flies where L1 and L2 were silenced together (brown) and their specific Gal4 control (gray), color-coded according to ON edge luminance. Sample sizes are n = 9 (*L1^{c2025},L2^{21Dhh}>>shi^{ts}*) and n = 8 (*L1^{c2025}-Gal4/+;L2^{21Dhh}-Gal4/+*). (D) Peak velocities quantified for each of the five edges during the motion period, ***p < 0.001, two-tailed Student's t tests against both controls. Traces and plots show mean ± SEM.

L1 is also an OFF pathway input

Given that three lamina neuron inputs encode visual stimuli differently and that all of them convey information to the ON-pathway, we next asked if L1 could also contribute to OFF-pathway function. To test this, we silenced L1 neurons while showing moving OFF edges, all of -100% contrast, and moving across five different background luminances. Control flies turned similarly under all conditions, showing lumiance-invariant responses (Figure 6A). Previous work showed that L3 is required to achieve luminance invariance by scaling behavioral responses when background luminance turned dark (Ketkar et al., 2020). Similarly, when L1 was silenced, behavioral responses were no longer invariant across luminance, but flies turned less to -100% contrast at low luminance as compared to high luminance (Figure 6A,B). Underestimation of the dim OFF stimuli by L1-silenced flies was not as strong as by L3-silenced flies (Ketkar et al., 2020), again highlighting the specialized role of L3 in dim light (Figure 6B). These data demonstrate that L1 luminance inputs are required for luminance-invariant OFF behavior. Since L1 carries both contrast and luminance information, it could be also sufficient to drive OFF behavior. To test this, we measured behavioral responses to OFF edges in L1 ort rescue flies. Heterozygous *ort* controls

showed turning responses to -100% OFF edges at five different luminances (Figure 6C). As described previously (Ketkar et al., 2020), *ort* null mutants were not completely blind to this OFF-edge motion stimulus and responded especially at high luminance but very little at low luminances. L1 ort rescue flies responded similarly to positive controls, rescuing OFF edges at low luminances (Figure 6D). Therefore, L1 is even sufficient to guide OFF behavior under the same conditions that were previously described for L3 (Ketkar et al., 2020). Taken together, these findings reveal that the lamina neurons L1 and L3 provide behaviorally relevant but differentially encoded luminance information to both ON and OFF pathways. In sum, our data uncover L1, L2 and L3 as important inputs for both ON and the OFF pathways, relevant for visually guided behaviors across luminances (Figure 6E).

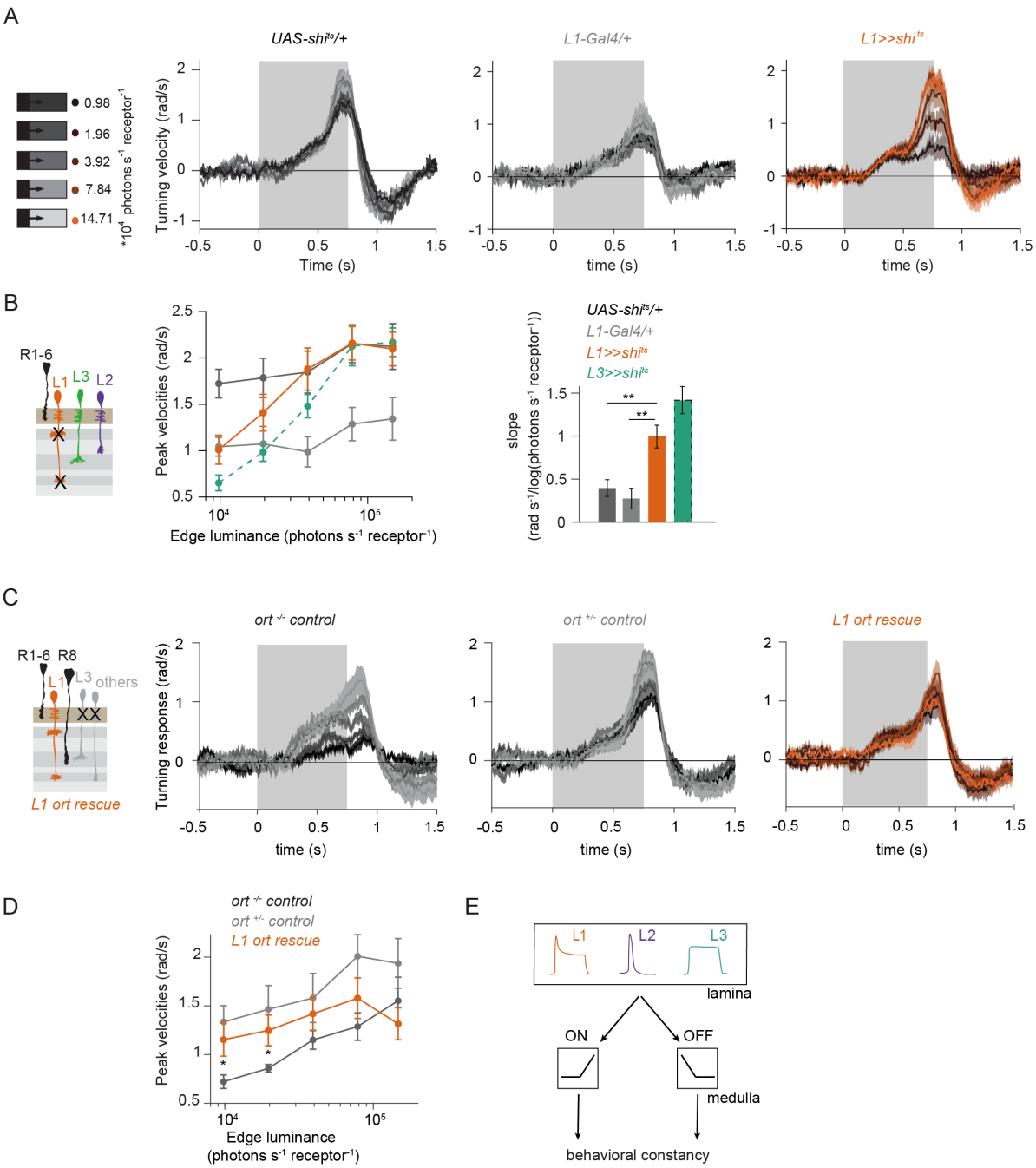

Figure 6: The L1 luminance signal is required and sufficient for OFF behavior. (A) Turning responses of L1-silenced flies (orange) and the controls (gray) to five OFF edges moving onto different backgrounds. (B) Peak velocities quantified for each of the five edges during the motion period, also including the peak velocities of L3-silenced flies (green dashed, re-quantified from the data in (Ketkar et al., 2020). Shown next to it is the relationship of the peak velocities with luminance, quantified as slopes of the linear fits to the data. **p < 0.01, two-tailed Student's t tests against both controls (not significant against the *L3>>shi^ts* slopes). Sample sizes are n = 7 *(L1-Gal4/+)* and n = 10 for other genotypes. (C) Schematics of the L1 ort rescue genotypes followed by its turning responses to the moving OFF edges. (D) Peak turning velocities of L1 ort rescue flies and the respective controls; *p<0.05, two-tailed Student's t tests against both controls. Sample sizes are n = 11 flies (*ort^-/-* control) and n =10 for other genotypes. The gray box region in (A) and (C) indicates motion duration. (E) Summary schematic. Lamina neurons L1-L3 distribute different visual features necessary for both ON and OFF pathways to guide contrast-constant behavior. Traces and plots show mean ± SEM.

Discussion

The present study establishes that contrast and luminance are basic visual features that interact with both ON and OFF pathways. In both pathways, the interaction between these features enables stable visual behaviors across changing conditions. The lamina neurons L1, L2 and L3 act as the circuit elements segregating both contrast and luminance information. Behavioral experiments show that luminance information is required for contrast constancy in both ON and OFF behaviors. While L1 and L3 provide contrast inputs to both ON and OFF pathways, L1 also encodes luminance, together with L3. Whereas L3 activity non-linearly increases with decreasing luminance, L1 shows a linear relationship with luminance. Luminance information from both neurons is differently used in ON and OFF pathways. Thus, L1, L2 and L3 are not ON or OFF pathways specific inputs, but they instead distribute the two most basic visual features, contrast and luminance, across pathways to enable behaviorally relevant computations.

Contrast constancy is a common feature of ON and OFF visual pathways, but with distinct implementations

Our work shows that visual behaviors guided by both ON and OFF pathways are luminance invariant. Similarly, luminance invariance has been shown in human perception of both ON and OFF contrasts, and in neural responses in cat LGN (Burkhardt et al., 1984; Mante et al., 2005). This argues that luminance invariance is a common feature of all visual systems, which is ethologically relevant for any species that relies on visual information for its survival in changing visual environments. Changing visual environments impose a common challenge onto the encoding of both ON and OFF contrasts, namely the contrasts are underestimated in sudden dim light. The L1 contrast-sensitive responses reflect such underestimation. Thus, both ON and OFF visual pathways would require a luminance-based correction to achieve luminance invariance, and such correction would in turn rely on luminance-sensitive neuronal signals themselves. We now confirm this hypothesis for both ON and OFF pathways. Specifically, luminance information from both L1 and L3 are required for luminance-invariant visual behaviors. However, the impact of the two neurons on behavior is pathway dependent. In the OFF pathway, losing either L1 or L3 function leads to a strong deviation from luminance invariance, such that the dim light stimuli are underestimated. On the contrary, ON motion-driven behavior only strongly deviates from invariance if both L1 and L3 neuron types are not functional. Furthermore, L2 neurons, which were formerly thought to be OFF pathway inputs, contribute contrast-sensitive information to ON behavior (Clark et al., 2011; Joesch et al., 2010; Silies et al., 2013). Notably, ON and OFF contrast constancy is not achieved symmetrically at every processing stage. For example, in the vertebrate retina, ON RGCs encode a mixture of luminance-invariant and absolute (i.e. luminance-dependent) contrast, whereas OFF RGCs encode predominantly absolute contrast (Idrees and Münch, 2020). Thus, asymmetrical implementation of contrast-corrective mechanisms can be common across visual systems, too.

All lamina neurons are inputs to both ON and OFF pathways

L1, L2 and L3 all show different contrast and luminance sensitivities. These distinct neuronal properties are then differentially utilized across ON and OFF pathways. How does this fit with the established notion that L1 is an input to the ON and L2 and L3 are inputs to OFF pathways? The luminance-varying stimuli sets used here were able to pull out lamina neuron contributions that were not obvious with simpler stimuli. For example, our data show that L1 and L2 provide redundant contrast input to the ON pathway at 100% contrast and varying luminance. However, L1 is still strictly required for ON responses if different contrasts are mixed. This is consistent with a more complex ON pathway input architecture and hints at a role for the L1 pathway in contrast adaptation. Interestingly, Mi1, an important post-synaptic partner of L1, shows an almost instantaneous and strong contrast adaptation (Matulis et al., 2020).

All three lamina neuron types hyperpolarize to light onset and depolarize to light offset and are not contrast selective themselves. Contrast selectivity emerges downstream of these neurons: known post-synaptic partners of L1 acquire ON contrast selectivity due to inhibitory glutamatergic synapses, whereas cholinergic L2 and L3 synapses retain OFF contrast selectivity (Molina-Obando et al., 2019). While L3 was actually already suggested to be an ON pathway input based on connectomics (Borst et al., 2020), other synaptic connections that link L1 to downstream OFF-selective neurons, and link L2 and to downstream ON-selective neurons still have to be investigated in detail. However, it now becomes evident that a split in ON and OFF circuitry only truly exists in downstream medulla neurons and direction-selective cells. The luminance and contrast features encoded differently in L1, L2 and L3 lamina neurons are shared by both pathways. Importantly, the distinct features that are passed on by the specific inputs downstream of photoreceptors guide distinct behavioral roles.

L1 and L3 convey luminance information to multiple pathways

Behavioral experiments in combination with genetic manipulations show that both L1 and L3 neurons provide luminance information to to achieve luminance-invariant behaviors. This functional data is consistent with anatomical predictions suggesting a role for L3 in the ON pathway based on synaptic contacts with ON-selective neurons (Takemura et al., 2013). L3 had mostly been considered an OFF pathway neuron because the OFF pathway neuron Tm9 receives its strongest input from L3 (Fisher et al., 2015; Shinomiya et al., 2014; Takemura et al., 2013). Remarkably, L3 itself actually makes most synaptic connections with the ON-pathway neuron Mi9. Further synapses of L3 with the ON-selective Mi1 neuron are similar in number to those with Tm9 (Takemura et al., 2013). Finally, L3 can potentially also convey information to the chromatic pathway, as Tm20 is its second strongest postsynaptic connection (Lin et al., 2016). There, L3 luminance sensitivity might play a relevant role in achieving color constancy, i.e., color recognition irrespective of illumination conditions. Altogether, anatomical and functional data indicate that it is time to redefine L3 as part of a luminance-encoding system rather than a mere OFF-pathway input.

A role of L1 beyond the ON pathway was less obvious based on anatomical data but is supported by functional connectivity studies showing that Tm9 properties rely in part on L1 input (Fisher et al., 2015), and that Tm9 together with other OFF pathway interneurons displays contrast-opponent receptive fields, adding evidence to the presence of ON information in the OFF pathway (Ramos-Traslosheros and Silies, 2021). Connectomics data did not identify any known OFF-

pathway neurons postsynaptic to L1 and presynaptic to the OFF-motion selective neuron T5 (Takemura et al., 2013). L1 must therefore connect to the OFF pathway via interneurons. Among the strongest postsynaptic partners of L1 are the GABAergic interneurons C2 and C3 that connect to the OFF pathway (Takemura et al., 2013). Intercolumnar neurons downstream of L1, such as Dm neurons (Nern et al., 2015), could further carry information to OFF-selective neurons, likely through disinhibition from ON-selective inputs. In the vertebrate retina, intercolumnar amacrine cells mediate interaction between ON and OFF bipolar cells, which has been shown to extend the operating range of the OFF pathway (Manookin et al., 2008; Odermatt et al., 2012). Altogether, strategies appear to be shared across animals in which type of interneurons help to convey relevant features from one pathway to the other.

Neurons postsynaptic to photoreceptors encode contrast and luminance differently

Despite being postsynaptic to the same photoreceptor input, all lamina neurons respond differently to light stimuli. L1 was previously considered the ON pathway sibling of the contrast-sensitive L2, both with regard to its temporal filtering properties and at the transcriptome level (Clark et al., 2011; Tan et al., 2015). However, L1 calcium signals show a transient and a sustained response component, which are contrast- and luminance-sensitive, respectively. Compared to photoreceptors, which also carry both contrast and luminance components, L1 still amplifies the contrast signals received from the photoreceptors, since its transient component is more pronounced than the one seen in the photoreceptor calcium traces (Gür et al., 2020). In other insect species, different types of lamina neurons have also been distinguished based on their physiological properties (Rusanen et al., 2018, 2017), although their specific luminance and contrast sensitivities are yet unknown.

The two luminance-sensitive neurons L1 and L3 differ in their luminance-encoding properties. L1's initial transient contrast response might reduce the operating range of the subsequent luminance-sensitive baseline. L3's calcium responses show little adaptation and can utilize most of its operating range to encode luminance. L3 seems to invest this wider operating range into amplifying the darkest luminance values selectively and non-linearly. Thus, a predominantly luminance-sensitive channel among LMCs may have evolved to selectively process stimuli in the low luminance range. The different linear and non-linear properties of L1 and L3 might further increase the dynamic range of luminance signaling (Odermatt et al., 2012). Together with the pure contrast sensitivity of L2, the first-order interneurons in flies exhibit a wide range of sensitivities with respect to contrast and luminance, and our data confirm the functional relevance of the differential sensitivities. Diversifying feature encoding through distinct temporal properties of first-order interneurons is a strategy employed to reliably handle wide luminance ranges.

Similarities and differences of peripheral processing strategies across species

In flies, three first-order interneurons feed contrast and luminance information into downstream circuitry. In the mouse retina, more than 30 functionally distinct bipolar types show a spectrum of temporal filter properties rather than a strict transient-sustained dichotomy, thus capturing a larger diversity of temporal information in parallel channels (e.g., (Baden et al., 2016; Ichinose et al.,

2014; Odermatt et al., 2012)). Many bipolar cell types resemble L1, in that they have both luminance and contrast signals in distinct response components (e.g., (Oesch and Diamond, 2011)). However, the degree of transiency varies from cell type to cell type, and some predominantly sustained bipolar cell types are also found, closely resembling the luminance-sensitive L3 (e.g., (Awatramani and Slaughter, 2000; Ichinose et al., 2014)). Such diversification of feature extraction at the periphery has been shown to be computationally advantageous, especially when processing complex natural scenes (e.g. (Odermatt et al., 2012; Rieke and Rudd, 2009)). For example, during daylight, visual scenes can differ in intensity by 4 to 5 log units, whereas electrical signals in cone photoreceptors reach a dynamic range of only two orders of magnitude (Naka and Rushton, 1966; Normann and Perlman, 1979; Pouli et al., 2010; Schnapf et al., 1990).

Although the vertebrate retina apparently has a much larger diversity of cell types to handle the wide and complex statistics of the visual environments, there is only a single layer of processing between photoreceptors and the first direction-selective cells, whereas in insects, there are two: the lamina and the medulla. It seems as if the combined properties of bipolar cells are spread across these two processing stages in the fly visual system: whereas some properties, such as diversity of temporal filtering starts in LMCs, contrast selectivity only emerges in medulla neurons and not directly in the first-order interneurons as it happens in bipolar cells. In both vertebrates and invertebrates, the emergence of ON selectivity occurs through inhibitory glutamatergic synapses, but whereas this happens at the photoreceptor-to-bipolar cell synapse in vertebrates, it happens one synapse further down between lamina and medulla neurons in flies (Masu et al., 1995; Molina-Obando et al., 2019). Taken together, LMCs and downstream medulla neurons combined appear to be the functional equivalents of vertebrate bipolar cell layers. Given the size limitations of the fly visual system to encode the same complex environment effectively, one benefit of this configuration with an extra layer could be that it allows more combinations. Furthermore, the photoreceptor-to-lamina synapse in the fly superposition eye already serves to spatially pool information from different photoreceptors (Braitenberg, 1967; Clandinin and Zipursky, 2002; Kirschfeld, 1967). In both visual systems, diversifying distinct information across several neurons could serve as a strategy to reliably respond to contrast when luminance conditions vary.

Methods

Experimental model

All flies were raised at 25 ºC and 65 % humidity on standard molasses-based fly food while being subjected to a 12:12h light-dark cycle. Two-photon experiments were conducted at room temperature (20 ºC) and behavioral experiments at 34 ºC. Female flies 2-4 days after eclosion were used for all experimental purposes. Lamina neuron driver lines used for genetic silencing and *ort* rescue experiments were *L3^{0595}-Gal4* (Silies et al., 2013), *L2^{21Dhh}-Gal4* and *L1^{C202a}-Gal4* (Rister et al., 2007), and *UAS-shi[ts], ort^{1},ninaE^{1}* and *Df(3R)BSC809* were from BDSC (# 44222, 1946 and 27380). Since the *ort^{1}* mutant chromosomes also carries a mutation in *ninaE^{1}* (*Drosophila rhodopsin1*), we used the *ort^{1}* mutation in trans to a deficiency that uncovers the *ort* but not the *ninaE* locus. *UAS-ort* was first described in (Hong et al., 2006). For imaging experiments, GCaMP6f (BDSC #42747) was expressed using *L1^{c202a}-Gal4*, *L2^{21Dhh}-Gal4* (Rister et al., 2007), and *L3^{MH56}-Gal4* (Timofeev et al., 2012). Detailed genotypes are given in Table 1.

Table 1.: Genotypes used in this study.

Name	Genotype	Figure
Imaging		
L1>>GCaMP6f	*w+; L1^{c202a}-Gal4 / +; UAS-GCaMP6f / +*	Fig 1, 2
L2>>GCaMP6f	*w+; UAS-GCaMP6f / +; L2^{21Dhh}-Gal4 / +*	Fig 2
L3>>GCaMP6f	*w+; L3^{MH56}-Gal4 / +; UAS-GCaMP6f / +*	Fig 2
Behavior		
UAS-shibire^{ts} control	*w+; + / +; UAS-shi^{ts} / +*	Fig 2, 3,4, 5, 6, S1, S2
L3-Gal4 control	*w+; +/ +; L3^{0595}-Gal4 /+*	Fig 4
L3 silencing	*w+; +/ +; L3^{0595}-Gal4 /UAS- shi^{ts}*	Fig 4
L1-Gal4 control	*w+; L1^{c202a}-Gal4 / +; + /+*	Fig 3, 6, S1
L1 silencing	*w+; L1^{c202a}-Gal4 / +; + /UAS- shi^{ts}*	Fig 3, 6, S1
L1-Gal4, L3-Gal4 control	*w+; L1^{c202a}-Gal4 / +; L3^{0595}-Gal4 /+*	Fig 4
L1, L3 silencing	*w+; L1^{c202a}-Gal4 / +; L3^{0595}-Gal4 /UAS- shi^{ts}*	Fig 4
ort mutant	*w+; UAS-ort / +; ort^{1},ninaE^{1} / Df(3R)BSC809*	Fig 3, 4, 6
L3 ort +/- control	*w+; + / +; L3^{0595}-Gal4, ort^{1}, ninaE^{1} / +*	Fig 4
L3 ort rescue	*w+; UAS-ort / +; L3^{0595}-Gal4, ort^{1},ninaE^{1} / Df(3R)BSC809*	Fig 4

L1 ort +/- control	*w+; L1^{c202a}-Gal4 / +, ort^{1}, ninaE^{1} / +*	Fig 3, 6
L1 ort rescue	*w+; UAS-ort / +; L1[c202a]; ort^{1},ninaE^{1} / Df(3R)BSC809*	Fig 3, 6
L2-Gal4 control	*w+; + /+; L2^{21Dhh}-Gal4 / +*	Fig 5,S2
L2 silencing	*w+; + / +; L2^{21Dhh}-Gal4 /UAS- shi^{ts}*	Fig 5, S2
L1-Gal4, L2-Gal4 control	*w+; L1^{c202a}-Gal4 / +; L2^{21Dhh}-Gal4 /+*	Fig 5, S2
L1, L2 silencing	*w+; L1^{c202a}-Gal4 / +; L2^{21Dhh}-Gal4 /UAS- shi^{ts}*	Fig 5, S2

Behavioral experiments

Behavioral experiments were performed as described in (Ketkar et al., 2020). In brief, all experiments were conducted at 34 ºC, a restrictive temperature for *shibire^{ts}* (Kitamoto, 2001). Female flies were cold anesthetized and glued to the tip of a needle at their thorax using UV-hardened Norland optical adhesive. A 3D micromanipulator positioned the fly above an air-cushioned polyurethane ball (Kugel-Winnie, Bamberg, Germany), 6 mm in diameter, and located at the center of a cylindrical LED arena that spanned 192º in azimuth and 80º in elevation (Reiser and Dickinson, 2008). The LED panels arena (IO Rodeo, CA, USA) consisted of 570 nm LEDs and was enclosed in a dark chamber. The pixel resolution was ~2º at the fly's elevation. Rotation of the ball was sampled at 120 Hz with two wireless optical sensors (Logitech Anywhere MX 1, Lausanne, Switzerland), positioned toward the center of the ball and at 90º to each other (setup described in (Seelig et al., 2010). Custom written C#-code was used to acquire ball movement data. MATLAB (Mathworks, MA, USA) was used to coordinate stimulus presentation and data acquisition. Data for each stimulus sequence were acquired for 15-20 minutes, depending on the number of distinct epochs in the sequence (see 'visual stimulation' for details).

Visual stimulation for behavior

The stimulation panels consist of green LEDs that can show 16 different, linearly spaced intensity levels. To measure the presented luminance, candela/m^2 values were first measured from the position of the fly using a LS-100 luminance meter (Konika Minolta, NJ, USA). Then, these values were transformed to photons incidence per photoreceptor per second, following the procedure described by (Dubs et al., 1981). The highest native LED luminance was approximately 11.77 * 10^5 photons * s^{-1} * photoreceptor^{-1} (corresponding to a measured luminance of 51.34 cd/m2), and the luminance meter read 0 candela/ m^2 when all LEDs were off. For all experiments, a 0.9 neutral

density filter foil (Lee filters) was placed in front of the panels, such that the highest LED level corresponded to 14.71 *10^4 photons*s^{-1}*$receptor^{-1}$.

Fly behavior was measured in an open-loop paradigm where either ON or OFF edges were presented. For every set of ON or OFF edges, each epoch was presented for around 60 to 80 trials. Each trial consisted of an initial static pattern (i.e., the first frame of the upcoming pattern) shown for 500 ms followed by 750 ms of edge motion. Inter-trial intervals were 1s. All edges from a set were randomly interleaved and presented in a mirror-symmetric fashion (moving to the right, or to the left) to account for potential biases in individual flies or introduced when positioning on the ball.

The ON edge stimuli comprised four edges, each covering 48º arena space. All ON edges moved with the angular speed of 160º/s. Thus, within a 750 ms stimulus epoch, the edge motion repeated thrice: After each repetition, the now bright arena was reset to the pre-motion lower LED level, and the next repetition followed immediately, picking up from the positions where the edges terminated in the first repetition. This way, each edge virtually moved continuously. The following sets of ON edges were presented:

1. 100% contrast edges: Here, the edges were made of 5 different luminance values (i.e. five unique epochs), moving on a complete dark background. Thus, the pre-motion LED level was zero, and the edges assumed the intensities 7%, 14%, 27%, 53% or 100% of the highest LED intensity (corresponding to the luminances: 0.98, 1.96, 3.92, 7.84 or 14.71 *10^4 photons*s^{-1}*$receptor^{-1}$ luminance). Thus, every epoch comprised 100% Michelson contrast. The inter-trial interval consisted of a dark screen.
2. Mixed-contrast edges – full range: The set comprised of seven distinct epochs, each with a different Michelson contrast value (11%, 25%, 33%, 43%, 67%, 82% and 100%). Here, the edge luminance was maintained constant at 67% of the highest LED intensity, across epochs, and the background luminance varied. The inter-trial interval showed a uniformly lit screen with luminance equivalent to the edge luminance.
3. Mixed-contrast edges – low contrast range: The set comprised of four distinct epochs, with contrasts from the range 9%, 18%, 27% and 36%. Here, edge luminances and background luminances both varied: The edge luminances assumed the intensities 80%, 87%, 93% and 100% of the highest LED intensity, whereas the background intensities were 67%, 60%, 53% and 47% of the highest LED intensity, respectively. The inter-trial interval consisted of a dark screen.

For the experiments concerning OFF edges, a set of five OFF edges comprising 100% Weber contrast was used as described in (Ketkar et al., 2020). Epoch consisted of a single OFF edge presented at one of five different uniformly lit backgrounds. The edge luminance was always ~zero, whereas the five different background luminances were 7%, 14%, 27%, 54% and 100% of the highest LED intensity (corresponding to five different background luminances: 0.98, 1.96, 3.92, 7.84 or 14.71 *10^4 photons*s^{-1}*$receptor^{-1}$). The inter-trial interval consisted of a dark screen.

Behavioral data analysis

Fly turning behavior was defined as yaw velocities that were derived as described in (Seelig et al., 2010), leading to a positive turn when flies turned in the direction of the stimulation and to a negative turn in the opposite case. Turning elicited by the same epoch moving either to the right or to the left were aggregated to compute the mean response of the fly to that epoch. Turning responses are presented as angular velocities (rad/s) averaged across flies ± SEM. Peak velocities were calculated over the stimulus motion period (750ms), shifted by 100 ms to account for a response delay, and relative to a baseline defined as the last 200 ms of the preceding inter-stimulus intervals. For the moving edges of 100% contrast and varying luminance, relation between peak velocities and luminance was assessed by fitting a straight line (V = a*log(luminance) + b) to the peak velocities of individual flies and quantifying the mean slope (a) ± SEM across flies. When comparing the slopes computed for behavior and L1 physiology, the two data types were first normalized for individual flies for behavior and individual regions of interest (ROIs) for L1 physiology (Figure 1E). For the *ort* rescue experiments, rescue efficiency was calculated at each stimulus luminance as

$$E_{rescue} = \frac{rescue - control^{-}}{control^{+} - control^{-}}$$

where E_{rescue} is the fractional rescue efficiency, *rescue* is the mean peak velocity of the rescue genotype such as L1 rescue, $control^{-}$ is the mean peak velocity of the *ort* null mutant negative control and $control^{+}$ stands for the mean peak velocity of the positive heterozygous ort^{1} control (e.g., *L1-Gal4;* ort^{1}/+). Statistical significance of E_{rescue} differences was tested using a permutation test. Specifically, flies of the genotypes L1 ort rescue and L3 ort rescue were shuffled 1000 times and the difference between their rescue efficiencies was obtained each time. The difference values so obtained gave a probability distribution that approximated a normal distribution. The efficiency difference was considered significant when it corresponded to less than 5% probability on both tails of the distribution.

Mean turning of flies as well as the slopes from control and experimental genotypes were normal distributed as tested using a Kolmogorov-Smirnov test ($p > 0.05$). Two-tailed Student's t tests and Bonferroni-Holm correction were performed between genotypes. Data points were considered significantly different only when the experimental group significantly differed from both genetic controls. Flies with a baseline forward walking speed of less than 2 mm/s were discarded from the analysis. This resulted in rejection of approximately 25% of all flies.

Two-photon imaging

Female flies were anesthetized on ice before placing them onto a sheet of stainless-steel foil bearing a hole that fit the thorax and head of the flies. Flies they were head fixated using UV-sensitive glue (Bondic). The head of the fly was tilted downward, looking toward the stimulation screen and their back of the head was exposed to the microscope objective. To optically access the optic lobe, a small window was cut in the cuticle on the back of the head using sharp forceps. During imaging, the brain was perfused with a carboxygenated saline-sugar imaging solution composed of 103 mM NaCl, 3 mM KCl, 5 mM TES, 1 mM NaH2PO4, 4 mM MgCl2, 1.5 mM

CaCl2,10 mM trehalose, 10 mM glucose, 7 mM sucrose, and 26 mM NaHCO3. Dissections were done in the same solution, but lacking calcium and sugars. The pH of the saline equilibrated near 7.3 when bubbled with 95% O2 / 5% CO2. The two-photon experiments for Figure 2 were performed using a Bruker Investigator microscope (Bruker, Madison,WI, USA), equipped with a 25x/NA1.1 objective (Nikon, Minato, Japan). An excitation laser (Spectraphysics Insight DS+) tuned to 920 nm was used to excite GCaMP6f, applying 5-15 mW of power at the sample. For experiments in Figure 1, a Bruker Ultima microscope, equipped with a 20x/NA1.0 objective (Leica, Jerusalem, Israel) was used. Here the excitation laser (YLMO-930 Menlo Systems, Martinsried, Germany) had a fixed 930 nm wavelength, and a power of 5-15 mW was applied at the sample.

In both setups, emitted light was sent through a SP680 shortpass filter, a 560 lpxr dichroic filter and a 525/70 emission filter. Data was acquired at a frame rate of ~10 to 15Hz and around 6–8x optical zoom, using PrairieView software.

Visual stimulation for imaging

For the staircase stimuli and light flashes of different luminances, the visual stimuli were generated by custom-written software using C++ and OpenGL and projected onto an 8cm x 8cm rear projection screen placed anterior to the fly and covering 60º of the fly's visual system in azimuth and 60º in elevation. These experiments were performed with the Bruker Investigator microscope.

For ON-moving edges, the stimulus was generated by custom-written software using the Python package PsychoPy (Peirce, 2008), and then projected onto a 9cm x 9cm rear projection screen placed anterior to the fly at a 45º angle and covering 80º of the fly's visual system in azimuth and 80º in elevation. These experiments were performed with the Bruker Ultima microscope.

Both stimuli were projected using a LightCrafter (Texas Instruments, Dallas, TX, USA), updating stimuli at a frame rate of 100 Hz. Before reaching the fly eye, stimuli were filtered by a 482/18 band pass filter and a ND1.0 neutral density filter (Thorlabs). The luminance values are measured using the same procedure described above for the behavioral experiments. The maximum luminance value measured at the fly position was $2.17*10^5$ photons s^{-1} $photoreceptor^{-1}$ for the staircase and random luminance stimulation, and $2.4*10^5$ photons s^{-1} $photoreceptor^{-1}$ for the ON-moving edge stimulation. The imaging and the visual stimulus presentation were synchronized as described previously (Freifeld et al., 2013).

Staircase stimulation

The stimulus consisted of 10s full-field flashes of 5 different luminances (0, 0.25, 0.5, 0.75 and 1_* of the maximal luminance I_{max}). The different luminance epochs were presented first in an increasing order (from darkness to full brightness) then in a decreasing order (full brightness to darkness). This sequence was repeated ~3-5 times.

Flashes of different luminances

The stimulus consisted of 10s full-field flashes of 5 different luminances (0, 0.25, 0.5, 0.75 and 1* of the maximal luminance I_{max}). The order between the flashes was pseudo-randomized and the stimulus sequence was presented for ~300s.

ON moving edges at different luminances

Here, the edges were made of 6 different luminance values (corresponding to 0.16, 0.31, 0.62, 1.2, 1.8, 2.4 $*10^5$ photons$*s^{-1}*$receptor^{-1} luminance), moving on a dark background. The inter-stimulus interval was 4 seconds of darkness.

Two photon data analysis

Staircase stimulation and randomized flashes of different luminances

Data processing was performed offline using MATLAB R2019a (The MathWorks Inc., Natick, MA). To correct for motion artifacts, individual images were aligned to a reference image composed of a maximum intensity projection of the first 30 frames. The average intensity for manually selected ROIs was computed for each imaging frame and background subtracted to generate a time trace of the response. All responses and visual stimuli were interpolated at 10 Hz and trial averaged. Neural responses are shown as relative fluorescence intensity changes over time (ΔF/F0). To calculate ΔF/F0, the mean of the whole trace was used as F0. In some recordings, a minority of ROIs responded in opposite polarity (positively correlated with stimulus), as described previously (Fisher et al., 2015). These ROIs have their receptive fields outside the stimulation screen (Fisher et al., 2015; Freifeld et al., 2013). To discard these and other noisy ROIs, we only used ROIs that were negatively correlated (Spearman's rank correlation coefficient) with the stimulus. Plateau responses were calculated as the mean of the last 2 seconds within each luminance presentation. In the randomized flashes of different luminances, plateau response values of the highest luminance epoch were subtracted for each plateau response to get a comparable relationship between each neuron for visualization (this leads to 0 plateau response for each neuron in the highest luminance condition). Mutual information between luminance and response was calculated according to (Ross, 2014). To characterize the distinct luminance-response relationships of L1 and L3, the difference of Pearson correlation and Spearman's rank correlation was used as a Non-linearity index. This value will reach zero if there is a strict linear relationship between luminance and response.

ON moving edges at different luminances

Data processing was performed offline using Python 2.7 (Van Rossum 1995). Motion correction was performed using the SIMA Python package's Hidden Markov Model based motion correction algorithm (Kaifosh et al., 2014). The average intensity for manually selected ROIs was computed for each imaging frame and background subtracted to generate a time trace of the response. To calculate ΔF/F0, the mean of the whole trace was used as F0. The traces were then trial averaged. Responses of ROIs for each epoch was calculated as the absolute difference between the mean

of the full darkness background epoch and the minimum of the ON edge presentation (minimum values are chosen because L1 neurons respond to ON stimuli with hyperpolarization).

Statistics

Throughout the analysis procedure, mean of quantified variables were calculated first for all ROIs within a fly, and then between flies. All statistical analysis was performed between flies. For normally distributed data sets, a two-tailed Student *t* test for unpaired (independent) samples was used. For other data sets, Wilcoxon rank-sum was used for statistical analysis. Normality was tested using Lilliefors test ($p>0.05$). One way ANOVA was used followed by multiple comparisons using the Bonferroni method for determining statistical significance between pairs of groups.

Acknowledgments

We thank members of the Silies lab for comments on the manuscript. We are grateful to Christine Gündner, Simone Renner, and Jonas Chojetzki for excellent technical assistance.
This project has received funding from the European Research Council (ERC) under the European Union's Horizon 2020 research and innovation program (grant agreement No 716512), and from the German Research Foundation (DFG) through the Emmy-Noether program (SI 1991/1-1) and the collaborative research center 1080 "Neural homeostasis" (project C06) to MS, as well as DFG grant MA 7804/2-1 to CM.

Author contributions:
Conceptualization: MK, BG, SMO and MS
Methodology: MK, BG, CM
Software: MK, BG, SMO
Investigation: MK, BG, SMO, MI
Visualization: MK, BG, SMO
Supervision: MS, CM
Writing—original draft: MK, SMO, MS
Writing—review & editing: all authors
Funding acquisition: MS

Competing interest:
The authors declare no competing interests.

Bibliography

Awatramani GB, Slaughter MM. 2000. Origin of Transient and Sustained Responses in Ganglion Cells of the Retina. *J Neurosci* **20**:7087–7095. doi:10.1523/JNEUROSCI.20-18-07087.2000

Baden T, Berens P, Franke K, Román Rosón M, Bethge M, Euler T. 2016. The functional diversity of retinal ganglion cells in the mouse. *Nature* **529**:345–350. doi:10.1038/nature16468

Behnia R, Clark DA, Carter AG, Clandinin TR, Desplan C. 2014. Processing properties of on and off pathways for Drosophila motion detection. *Nature*. doi:10.1038/nature13427

Borst A, Haag J, Mauss AS. 2020. How fly neurons compute the direction of visual motion. *J Comp Physiol A* **206**:109–124. doi:10.1007/s00359-019-01375-9

Braitenberg V. 1967. Patterns of projection in the visual system of the fly. I. Retina-lamina projections. *Exp Brain Res* **3**:271–298. doi:10.1007/BF00235589

Burkhardt DA, Gottesman J, Kersten D, Legge GE. 1984. Symmetry and constancy in the perception of negative and positive luminance contrast. *J Opt Soc Am A* **1**:309. doi:10.1364/JOSAA.1.000309

Chichilnisky EJ, Kalmar RS. 2002. Functional Asymmetries in ON and OFF Ganglion Cells of Primate Retina. *J Neurosci* **22**:2737–2747. doi:10.1523/JNEUROSCI.22-07-02737.2002

Clandinin TR, Zipursky SL. 2002. Making connections in the fly visual system. *Neuron* **35**:827–841. doi:10.1016/S0896-6273(02)00876-0

Clark DA, Bursztyn L, Horowitz MA, Schnitzer MJ, Clandinin TR. 2011. Defining the Computational Structure of the Motion Detector in Drosophila. *Neuron*. doi:10.1016/j.neuron.2011.05.023

Clark DA, Demb JB. 2016. Parallel Computations in Insect and Mammalian Visual Motion Processing. *Curr Biol* **26**:R1062–R1072. doi:10.1016/j.cub.2016.08.003

Clark DA, Fitzgerald JE, Ales JM, Gohl DM, Silies MA, Norcia AM, Clandinin TR. 2014. Flies and humans share a motion estimation strategy that exploits natural scene statistics. *Nat Neurosci* **17**:296–303. doi:10.1038/nn.3600

Dubs A, Laughlin SB, Srinivasan MV. 1981. Single photon signals in fly photoreceptors and first order interneurones at behavioral threshold. *J Physiol* **317**:317–334. doi:10.1113/jphysiol.1981.sp013827

Euler T, Haverkamp S, Schubert T, Baden T. 2014. Retinal bipolar cells: Elementary building blocks of vision. *Nat Rev Neurosci* **15**:507–519. doi:10.1038/nrn3783

Fischbach KF, Dittrich APM. 1989. The optic lobe of Drosophila melanogaster. I. A Golgi analysis of wild-type structure. *Cell Tissue Res*. doi:10.1007/BF00218858

Fisher YE, Leong JCS, Sporar K, Ketkar MD, Gohl DM, Clandinin TR, Silies M. 2015. A Class of Visual Neurons with Wide-Field Properties Is Required for Local Motion Detection. *Curr Biol*. doi:10.1016/j.cub.2015.11.018

Frazor RA, Geisler WS. 2006. Local luminance and contrast in natural images. *Vision Res* **46**:1585–1598. doi:10.1016/j.visres.2005.06.038

Freifeld L, Clark DA, Schnitzer MJ, Horowitz MA, Clandinin TR. 2013. GABAergic Lateral Interactions Tune the Early Stages of Visual Processing in Drosophila. *Neuron*. doi:10.1016/j.neuron.2013.04.024

Gür B, Sporar K, Lopez-Behling A, Silies M. 2020. Distinct expression of potassium channels regulates visual response properties of lamina neurons in Drosophila melanogaster. *J Comp Physiol A Neuroethol Sens Neural Behav Physiol* **206**:273–287. doi:10.1007/s00359-019-01385-7

Hong S-T, Bang S, Paik D, Kang J, Hwang S, Jeon K, Chun B, Hyun S, Lee Y, Kim J. 2006. Histamine and Its Receptors Modulate Temperature-Preference Behaviors in Drosophila. *J Neurosci* **26**:7245–7256. doi:10.1523/JNEUROSCI.5426-05.2006

Ichinose T, Fyk-Kolodziej B, Cohn J. 2014. Roles of ON Cone Bipolar Cell Subtypes in Temporal Coding in the Mouse Retina. *J Neurosci* **34**:8761–8771. doi:10.1523/JNEUROSCI.3965-13.2014

Ichinose T, Hellmer CB. 2016. Differential signalling and glutamate receptor compositions in the OFF bipolar cell types in the mouse retina: Temporal coding in the retinal OFF bipolar cells. *J Physiol* **594**:883–894. doi:10.1113/JP271458

Ichinose T, Lukasiewicz PD. 2007. Ambient Light Regulates Sodium Channel Activity to Dynamically Control Retinal Signaling. *J Neurosci* **27**:4756–4764. doi:10.1523/JNEUROSCI.0183-07.2007

Idrees S, Münch TA. 2020. Different contrast encoding in ON and OFF visual pathways (preprint). Neuroscience. doi:10.1101/2020.11.25.398230

Jin J, Wang Y, Lashgari R, Swadlow HA, Alonso J-M. 2011. Faster Thalamocortical Processing for Dark than Light Visual Targets. *J Neurosci* **31**:17471–17479. doi:10.1523/JNEUROSCI.2456-11.2011

Joesch M, Plett J, Borst A, Reiff DF. 2008. Response Properties of Motion-Sensitive Visual Interneurons in the Lobula Plate of Drosophila melanogaster. *Curr Biol* **18**:368–374. doi:10.1016/j.cub.2008.02.022

Joesch M, Schnell B, Raghu SV, Reiff DF, Borst A. 2010. ON and off pathways in Drosophila motion vision. *Nature*. doi:10.1038/nature09545

Kaifosh P, Zaremba JD, Danielson NB, Losonczy A. 2014. SIMA: Python software for analysis of dynamic fluorescence imaging data, Frontiers in Neuroinformatics.

Ketkar MD, Sporar K, Gür B, Ramos-Traslosheros G, Seifert M, Silies M. 2020. Luminance Information Is Required for the Accurate Estimation of Contrast in Rapidly Changing Visual Contexts. *Curr Biol*. doi:10.1016/j.cub.2019.12.038

Kirschfeld K. 1967. Die projektion der optischen umwelt auf das raster der rhabdomere im komplexauge von Musca. *Exp Brain Res* **3**:248–270. doi:10.1007/BF00235588

Kitamoto T. 2001. Conditional modification of behavior inDrosophila by targeted expression of a temperature-sensitiveshibire allele in defined neurons. *J Neurobiol* **47**:81–92. doi:10.1002/neu.1018

Laughlin SB, Hardie RC. 1978. Common strategies for light adaptation in the peripheral visual systems of fly and dragonfly. *J Comp Physiol* **128**:319–340. doi:10.1007/BF00657606

Leonhardt A, Ammer G, Meier M, Serbe E, Bahl A, Borst A. 2016. Asymmetry of Drosophila on and off motion detectors enhances real-world velocity estimation. *Nat Neurosci*. doi:10.1038/nn.4262

Lin T-Y, Luo J, Shinomiya K, Ting C-Y, Lu Z, Meinertzhagen IA, Lee C-H. 2016. Mapping chromatic pathways in the *Drosophila* visual system: Chromatic Visual Circuits in the Fly's Lobula. *J Comp Neurol* **524**:213–227. doi:10.1002/cne.23857

Manookin MB, Beaudoin DL, Ernst ZR, Flagel LJ, Demb JB. 2008. Disinhibition Combines with Excitation to Extend the Operating Range of the OFF Visual Pathway in Daylight. *J Neurosci* **28**:4136–4150. doi:10.1523/JNEUROSCI.4274-07.2008

Mante V, Frazor RA, Bonin V, Geisler WS, Carandini M. 2005. Independence of luminance and contrast in natural scenes and in the early visual system. *Nat Neurosci* **8**:1690–1697. doi:10.1038/nn1556

Masu M, Iwakabe H, Tagawa Y, Miyoshi T, Yamashita M, Fukuda Y, Sasaki H, Hiroi K, Nakamura Y, Shigemoto R. 1995. Specific deficit of the ON response in visual transmission by targeted disruption of the mGluR6 gene. *Cell* **80**:757–765.

Matulis CA, Chen J, Gonzalez-Suarez AD, Behnia R, Clark DA. 2020. Heterogeneous Temporal Contrast Adaptation in Drosophila Direction-Selective Circuits. *Curr Biol*. doi:10.1016/j.cub.2019.11.077

Mauss AS, Vlasits A, Borst A, Feller M. 2017. Visual Circuits for Direction Selectivity. doi:10.1146/annurev-neuro-072116

Meinertzhagen IA, O'Neil SD. 1991. Synaptic organization of columnar elements in the lamina of the wild type in Drosophila melanogaster. *J Comp Neurol* **305**:232–263. doi:10.1002/cne.903050206

Molina-Obando S, Vargas-Fique JF, Henning M, Gür B, Schladt M, Akhtar J, Berger TK, Silies M. 2019. ON selectivity in the Drosophila visual system is a multisynaptic process involving both glutamatergic and GABAergic inhibition. doi:10.7554/eLife.49373.001

Naka KI, Rushton WAH. 1966. S-potentials from luminosity units in the retina of fish (Cyprinidae). *J Physiol* **185**:587–599. doi:10.1113/jphysiol.1966.sp008003

Nern A, Pfeiffer BD, Rubin GM. 2015. Optimized tools for multicolor stochastic labeling reveal diverse stereotyped cell arrangements in the fly visual system. *Proc Natl Acad Sci* **112**:E2967–E2976. doi:10.1073/pnas.1506763112

Normann RA, Perlman I. 1979. The effects of background illumination on the photoresponses of red and green cones. *J Physiol* **286**:491–507. doi:10.1113/jphysiol.1979.sp012633

Normann RA, Werblin FS. 1974. Control of Retinal Sensitivity I . Light and Dark Adaptation of. *J Gen Physiol* **63**:37–61. doi:10.1085/jgp.63.1.37

Odermatt B, Nikolaev A, Lagnado L. 2012. Encoding of Luminance and Contrast by Linear and Nonlinear Synapses in the Retina. *Neuron* **73**:758–773. doi:10.1016/j.neuron.2011.12.023

Oesch NW, Diamond JS. 2011. Ribbon synapses compute temporal contrast and encode luminance in retinal rod bipolar cells. *Nat Neurosci* **14**:1555–1561. doi:10.1038/nn.2945

Peirce JW. 2008. Generating stimuli for neuroscience using PsychoPy. *Front Neuroinformatics* **2**. doi:10.3389/neuro.11.010.2008

Pouli T, Cunningham D, Reinhard E. 2010. Statistical regularities in low and high dynamic range imagesProceedings of the 7th Symposium on Applied Perception in Graphics and Visualization - APGV '10. Presented at the the 7th Symposium. Los Angeles, California: ACM Press. p. 9. doi:10.1145/1836248.1836250

Ramos-Traslosheros G, Silies M. 2021. The physiological basis for contrast opponency in motion computation in Drosophila. *Nat Commun* **12**:1–16. doi:10.1038/s41467-021-24986-w

Ratliff CP, Borghuis BG, Kao Y-H, Sterling P, Balasubramanian V. 2010. Retina is structured to process an excess of darkness in natural scenes. *Proc Natl Acad Sci* **107**:17368–17373. doi:10.1073/pnas.1005846107

Reiser MB, Dickinson MH. 2008. A modular display system for insect behavioral neuroscience. *J Neurosci Methods* **167**:127–139. doi:10.1016/j.jneumeth.2007.07.019

Rieke F, Rudd ME. 2009. The Challenges Natural Images Pose for Visual Adaptation. *Neuron* **64**:605–616. doi:10.1016/j.neuron.2009.11.028

Rister J, Pauls D, Schnell B, Ting CY, Lee CH, Sinakevitch I, Morante J, Strausfeld NJ, Ito K, Heisenberg M. 2007. Dissection of the Peripheral Motion Channel in the Visual System of Drosophila melanogaster. *Neuron* **56**:155–170. doi:10.1016/j.neuron.2007.09.014

Ross BC. 2014. Mutual information between discrete and continuous data sets. *PLoS ONE* **9**:e87357–e87357. doi:10.1371/journal.pone.0087357

Ruderman DL. 1994. The statistics of natural images. *Netw Comput Neural Syst* **5**:517–548. doi:10.1088/0954-898X_5_4_006

Rusanen J, Frolov R, Weckström M, Kinoshita M, Arikawa K. 2018. Non-linear amplification of graded voltage signals in the first-order visual interneurons of the butterfly Papilio xuthus. *J Exp Biol* **221**:jeb179085–jeb179085. doi:10.1242/jeb.179085

Rusanen J, Vähäkainu A, Weckström M, Arikawa K. 2017. Characterization of the first-order visual interneurons in the visual system of the bumblebee (Bombus terrestris). *J Comp Physiol A Neuroethol Sens Neural Behav Physiol* **203**:903–913. doi:10.1007/s00359-017-1201-9

Schnapf JL, Nunn BJ, Meister M, Baylor DA. 1990. Visual transduction in cones of the monkey Macaca fascicularis. *J Physiol* **427**:681–713. doi:10.1113/jphysiol.1990.sp018193

Seelig JD, Chiappe ME, Dutta A, Osborne JE, Reiser MB, Jayaraman V. 2010. Two-photon calcium imaging from head-fixed Drosophila during optomotor walking behavior. *Nat Methods* **7**:535–40. doi:10.1038/nmeth.1468

Serbe E, Meier M, Leonhardt A, Borst A. 2016. Comprehensive Characterization of the Major Presynaptic Elements to the Drosophila OFF Motion Detector. *Neuron* **89**:829–841. doi:10.1016/j.neuron.2016.01.006

Shapley R, Enroth-Cugell C. 1984. Chapter 9 Visual adaptation and retinal gain controls. *Prog Retin Res* **3**:263–346. doi:10.1016/0278-4327(84)90011-7

Shinomiya K, Huang G, Lu Z, Parag T, Xu CS, Aniceto R, Ansari N, Cheatham N, Lauchie S, Neace E, Ogundeyi O, Ordish C, Peel D, Shinomiya A, Smith C, Takemura S, Talebi I, Rivlin PK, Nern A, Scheffer LK, Plaza SM, Meinertzhagen IA. 2019. Comparisons between the ON- and OFF-edge motion pathways in the Drosophila brain. *eLife* **8**:e40025. doi:10.7554/eLife.40025

Shinomiya K, Karuppudurai T, Lin TY, Lu Z, Lee CH, Meinertzhagen IA. 2014. Candidate neural substrates for off-edge motion detection in drosophila. *Curr Biol*. doi:10.1016/j.cub.2014.03.051

Silies M, Gohl DM, Clandinin TR. 2014. Motion-Detecting Circuits in Flies: Coming into View. *Annu Rev Neurosci* **37**:307–327. doi:10.1146/annurev-neuro-071013-013931

Silies M, Gohl DM, Fisher YE, Freifeld L, Clark DA, Clandinin TR. 2013. Modular Use of Peripheral Input Channels Tunes Motion-Detecting Circuitry. *Neuron*. doi:10.1016/j.neuron.2013.04.029

Strother JA, Nern A, Reiser MB. 2014. Direct observation of on and off pathways in the drosophila visual system. *Curr Biol*. doi:10.1016/j.cub.2014.03.017

Strother JA, Wu ST, Wong AM, Nern A, Rogers EM, Le JQ, Rubin GM, Reiser MB. 2017. The Emergence of Directional Selectivity in the Visual Motion Pathway of Drosophila. *Neuron* **94**:168-182.e10. doi:10.1016/j.neuron.2017.03.010

Takemura Shin-ya, Bharioke A, Lu Z, Nern A, Vitaladevuni S, Rivlin PK, Katz WT, Olbris DJ, Plaza SM, Winston P, Zhao T, Horne JA, Fetter RD, Takemura Satoko, Blazek K, Chang LA, Ogundeyi O, Saunders MA, Shapiro V, Sigmund C, Rubin GM, Scheffer LK, Meinertzhagen IA, Chklovskii DB. 2013. A visual motion detection circuit suggested by Drosophila connectomics. *Nature*. doi:10.1038/nature12450

Takemura Shin-ya, Xu CS, Lu Z, Rivlin PK, Parag T, Olbris DJ, Plaza S, Zhao T, Katz WT, Umayam L, Weaver C, Hess HF, Horne JA, Nunez-Iglesias J, Aniceto R, Chang L-A, Lauchie S, Nasca A, Ogundeyi O, Sigmund C, Takemura Satoko, Tran J, Langille C, Lacheur KL, McLin S, Shinomiya A, Chklovskii DB, Meinertzhagen IA, Scheffer LK. 2015. Synaptic circuits and their variations within different columns in the visual system of Drosophila. *Proc Natl Acad Sci* **112**:13711–13716. doi:10.1073/pnas.1509820112

Takemura SY, Nern A, Chklovskii DB, Scheffer LK, Rubin GM, Meinertzhagen IA. 2017. The comprehensive connectome of a neural substrate for 'ON' motion detection in Drosophila. *eLife*. doi:10.7554/eLife.24394

Tan L, Zhang KX, Pecot MY, Nagarkar-Jaiswal S, Lee PT, Takemura SY, McEwen JM, Nern A, Xu S, Tadros W, Chen Z, Zinn K, Bellen HJ, Morey M, Zipursky SL. 2015. Ig Superfamily Ligand and Receptor Pairs Expressed in Synaptic Partners in Drosophila. *Cell* **163**:1756–1769. doi:10.1016/j.cell.2015.11.021

Timofeev K, Joly W, Hadjieconomou D, Salecker I. 2012. Localized netrins act as positional cues to control layer-specific targeting of photoreceptor axons in drosophila. *Neuron* **75**:80–93. doi:10.1016/j.neuron.2012.04.037

Yang HH, Clandinin TR. 2018. Elementary Motion Detection in Drosophila : Algorithms and Mechanisms. *Annu Rev Vis Sci* **4**:143–163. doi:10.1146/annurev-vision-091517-034153

955 Yang HHH, St-Pierre F, Sun X, Ding X, Lin MZZ, Clandinin TRR. 2016. Subcellular Imaging of
956 Voltage and Calcium Signals Reveals Neural Processing In Vivo. *Cell* **166**:245–257.
957 doi:10.1016/j.cell.2016.05.031
958

Supplementary figures

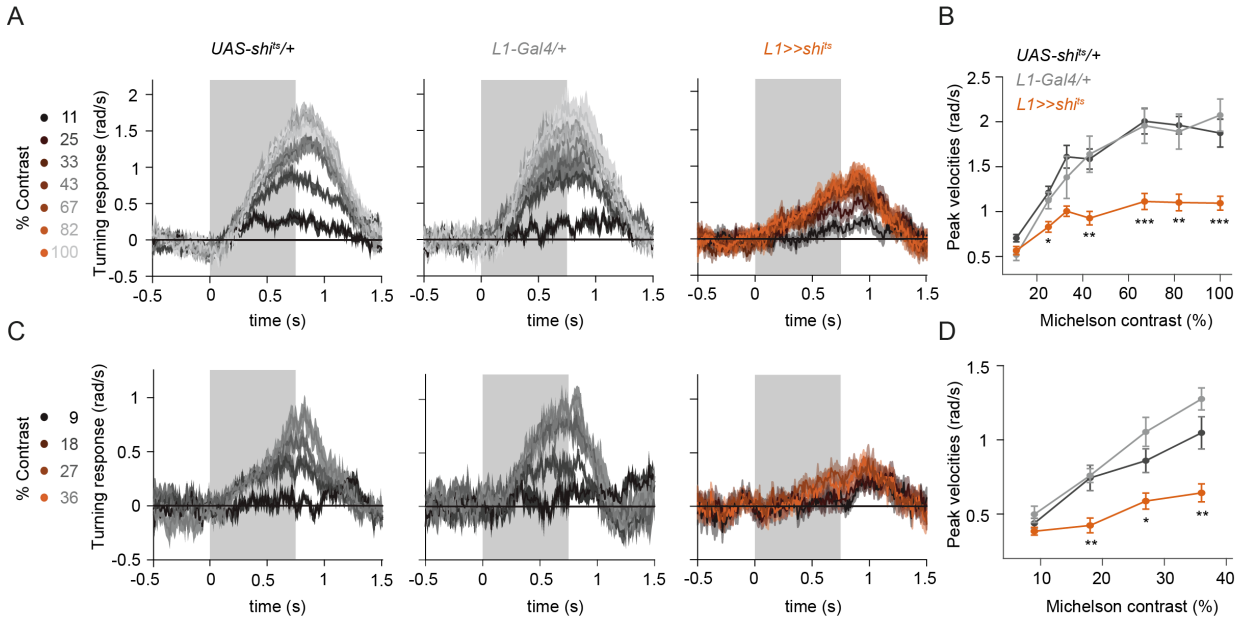

Figure S1: L1 is required for ON behavior across a range of contrasts. (A) Turning responses of the controls (gray) and L1-silenced flies (orange) in response to the moving ON edges of different contrasts, ranging from 11% to 100%. (B) Peak turning velocities quantified during the motion period, *p < 0.05, ***p < 0.01, ***p < 0.001, two-tailed Student's t tests against both controls. Sample sizes are n = 9 (*UAS-shi^{ts}/+, L1^{c202a} >>shi^{ts}*) and n = 5 (*L1^{c202a}-Gal4/+*). (C) Turning velocity time traces of the controls and L3-silenced flies in response to the moving ON edges of different contrasts, ranging from 9% to 36%. (D) Peak turning velocities quantified during the motion period, *p < 0.05, two-tailed Student's t tests against both controls. Sample sizes are n = 8 (*UAS-shi^{ts}/+),* n = 8 *(L1^{c202a} >>shi^{ts}*) and n = 5 (*L1^{c202a} -Gal4/+*). Traces and plots show mean ± SEM. The gray box region in (A) and (C) indicates motion duration.

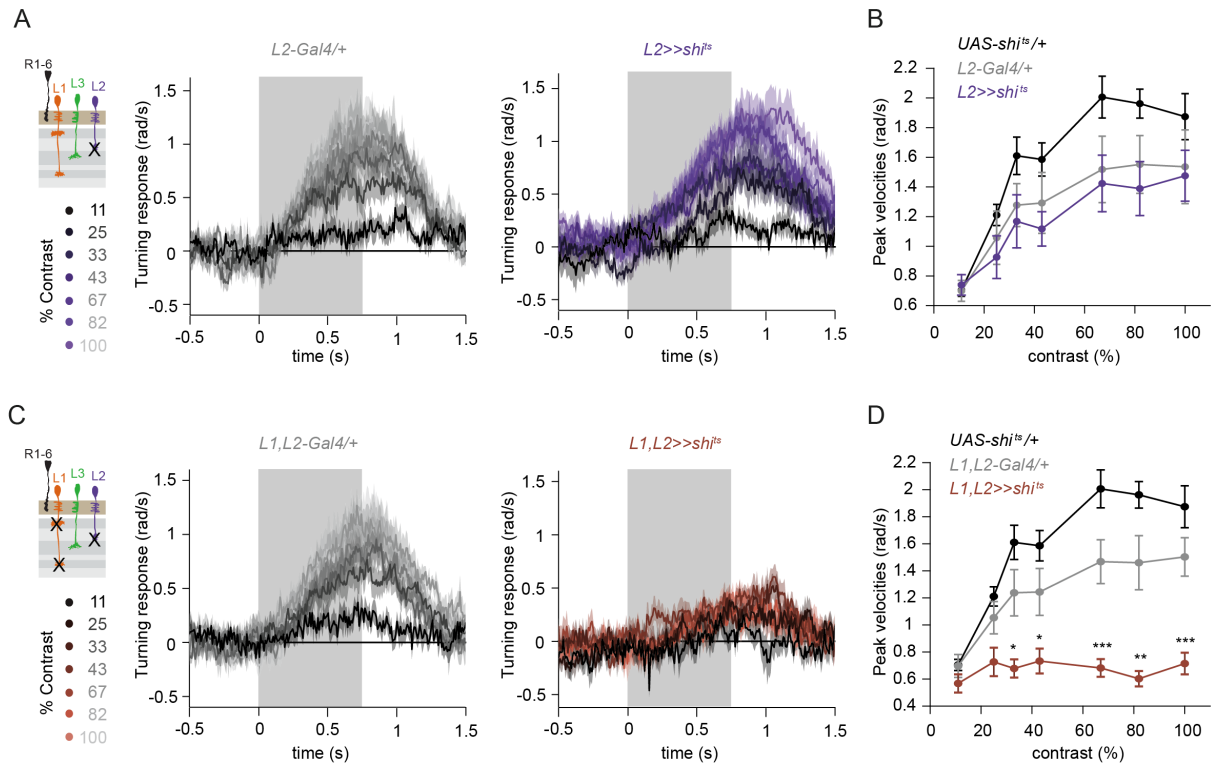

Figure S2: L1 and L2 together are required for ON behavior across a range of contrasts. (A) Turning velocity time traces of the Gal4 control (gray) and L2-silenced flies (purple) in response to the moving ON edges of different contrasts, ranging from 11% to 100%. (B) Peak turning velocities quantified during the motion period. Sample sizes are n = 9 (*UAS-shi^{ts}/+),* n = 8 *(L2^{21Dhh} >>shi^{ts}*) and n = 8 (*L2^{21Dhh}-Gal4/+*). (C) Turning velocity time traces of the Gal4 control and L1,L2-silenced flies (brown) in response to the moving ON edges of different contrasts, ranging from 11% to 100%. (D) Peak turning velocities quantified during the motion period, *p < 0.05, **p < 0.01, ***p < 0.001, two-tailed Student's t tests against both controls. Sample sizes are n = 9 (*UAS-shi^{ts}/+),*n = 8 *(L1,L2 >>shi^{ts}*) and n = 9 (*L1,L2 -Gal4/+*). Traces and plots show mean ± SEM. The gray box region in (A) and (C) indicates motion duration.

964